nature medicine

Muscle-specific *Pparg* deletion causes insulin resistance

Andrea L Hevener [1,6], Weimin He[1,6], Yaacov Barak[3,4,6], Jamie Le[1], Gautam Bandyopadhyay[1], Peter Olson[2,4], Jason Wilkes[1], Ronald M Evans[4,5] & Jerrold Olefsky[1]

Thiazolidinediones (TZDs) are insulin-sensitizing drugs and are potent agonists of the nuclear peroxisome proliferator-activated receptor-γ (PPAR-γ). Although muscle is the major organ responsible for insulin-stimulated glucose disposal, PPAR-γ is more highly expressed in adipose tissue than in muscle. To address this issue, we used the Cre-*lox*P system to knock out *Pparg*, the gene encoding PPAR-γ, in mouse skeletal muscle. As early as 4 months of age, mice with targeted disruption of PPAR-γ in muscle showed glucose intolerance and progressive insulin resistance. Using the hyperinsulinemic-euglycemic clamp technique, the *in vivo* insulin-stimulated glucose disposal rate (IS-GDR) was reduced by ~80% and was unchanged by 3 weeks of TZD treatment. These effects reveal a crucial role for muscle PPAR-γ in the maintenance of skeletal muscle insulin action, the etiology of insulin resistance and the action of TZDs.

Insulin resistance is a fundamental characteristic of most patients with type 2 diabetes, and is the defining feature of Metabolic Syndrome, or Syndrome X[1–3]. The discovery of TZDs as antidiabetic insulin sensitizers has had a major therapeutic and scientific impact[4–6]. TZDs are agonists for nuclear PPAR-γ and increase insulin sensitivity in cells, animals and humans[6–12]. PPAR-γ is expressed at high levels in adipose tissue, and its activation promotes differentiation of adipocytes and other cell types[9–32]. However, its expression in muscle is only 5–10% of its expression in fat[13,33]. PPAR-γ forms a heterodimer with the retinoid-X receptor and binds to PPAR response elements in the promoter domains of target genes[20,23]. PPAR-γ is thought to help maintain the proper levels of key glucoregulatory and lipogenic molecules[21].

Knocking out PPAR-γ by homologous recombination leads to embryonic lethality by E11, as a result of severe trophoblast dysmorphogenesis[34]. Tetraploid rescue of this defect reveals a second stage of lethality marked by total lipodystrophy[34]. The dominant function of PPAR-γ in adipocyte differentiation and the role of PPAR-γ as the molecular target for antidiabetic TZDs suggest a specific role for adipose tissue in the etiology of the disease. In this view, the antidiabetic effects observed in muscle are a consequence of the actions of these drugs in fat. This notion is supported by fact that PPAR-γ expression is high in fat and low in muscle.

Although the role of PPAR-γ in glucose and lipid metabolism is well documented, the tissue-specific effects of PPAR-γ expression and the crucial site(s) for TZD action remain unclear. We established a strain of mice with muscle-specific deletion of *Pparg*, the gene encoding PPAR-γ, using the Cre-*lox*P gene targeting system.

Here we report that deletion of *Pparg* in skeletal muscle caused severe insulin resistance in muscle, with milder defects observed in adipose tissue and liver. Furthermore, TZD treatment did not increase skeletal muscle insulin sensitivity in these animals. These findings show that muscle PPAR-γ expression has a crucial role in skeletal muscle insulin sensitivity and TZD action, and can exert indirect effects on insulin action in adipose tissue and liver.

RESULTS

Deletion of *Pparg* in skeletal muscle

We used Cre-*lox*P-mediated gene targeting to delete *Pparg* in skeletal and cardiac myocytes. Mice harboring *lox*P sites flanking exons 1 and 2 of *Pparg* were generated by homologous recombination (**Fig. 1a**,**b**) and used to produce two strains for this study: the homozygous $Pparg^{fl/fl}$ and the null heterozygous $Pparg^{fl/-}$. These were mated to a *Cre*-transgenic line (MCK-*Cre*; ref. 35) expressing Cre recombinase under the control of the muscle creatine kinase (MCK) promoter. Strains showing efficient Cre mRNA expression in muscle, but not in other organs or tissues, were expanded to produce muscle-specific *Pparg* deletions (muscle knockout, MKO) in the context of either normal ($MKO^{fl/fl}$) or haploinsufficient ($MKO^{fl/-}$) PPAR-γ expression in all other tissues. Control mice were fl/fl or fl/– littermates not expressing *Cre*. The metabolic phenotypes of these animals ($control^{fl/fl}$, $MKO^{fl/fl}$, $control^{fl/-}$ and $MKO^{fl/-}$) were assessed up to 14 months of age.

Examination of skeletal muscle from MKO mice revealed no gross abnormalities or obvious changes in cell size compared with muscle from $control^{fl/fl}$ or $control^{fl/-}$ littermates, although there was an ~50% increase in muscle triglyceride content in both groups of MKO mice (**Table 1**).

Pparg recombination in muscle results in major mRNA reduction

To quantitate the wild-type and recombined mRNA in muscle and non-muscle tissue, we designed primers that flank deleted exons 1

[1]Department of Medicine, Division of Endocrinology and Metabolism, University of California, San Diego, La Jolla, California 92093, USA. [2]Department of Biology, University of California, San Diego, La Jolla, California 92093, USA. [3]Jackson Laboratory, Bar Harbor, Maine 04609, USA. [4]Gene Expression Laboratory and [5]Howard Hughes Medical Institute, The Salk Institute, La Jolla, California 92093, USA. [6]These authors contributed equally to this work. Correspondence should be addressed to J.O. (jolefsky@ucsd.edu) or R.M.E. (evans@salk.edu).

Published online 16 November 2003; doi:10.1038/nm956

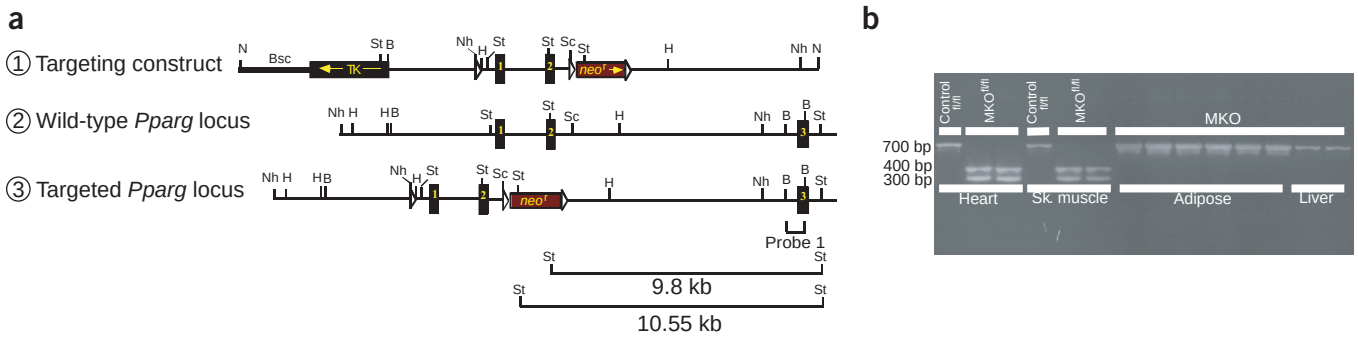

Figure 1 Floxed *Pparg* targeting construct and muscle gene deletion. (**a**) Construct design and recombination schematic. (1) Targeting construct to introduce *lox*P sites into *Pparg*. (2) Restriction map of *Pparg* exons 1 and 2. (3) *Pparg* after homologous recombination. Probe 1 indicates position of DNA fragment outside region of recombination used to identify homologous recombinant embryonic stem cell clones. (**b**) Detection of wild-type and mutant PPAR-γ mRNA by RT-PCR. Tissue RNA was isolated from white adipose tissue, heart, skeletal muscle and liver from the indicated mouse genotypes and subjected to RT-PCR. Arrows indicate detected wild-type (700 bp) and mutant (300 and 400 bp) PPAR-γ PCR products.

and 2, such that wild-type mRNA yields a product of 700 base pairs (bp) and recombined mRNA produces a 300- to 400-bp product. Only wild-type mRNA is detected in the non-muscle insulin target tissues (liver and adipose tissue; **Fig. 1b**). In skeletal and heart muscle from control$^{fl/fl}$ animals (which do not express Cre in muscle), only wild-type mRNA is present, with no detectable recombined bands. In contrast, very little, if any, wild-type mRNA can be detected in MKO$^{fl/fl}$ animals, whereas recombined bands are easily detected. The recombinant mRNA yields PCR products of both 300 and 400 bp. The 300-bp band has the exact sequence predicted from the deletion of the *lox*P-flanked region. The 400-bp product is identical to the 300-bp product, except that an additional 100 bp of intronic sequence from intron 3 of *Pparg* was spliced into this transcript.

Although wild-type PPAR-γ has been found in total muscle tissue, this is the first unambiguous demonstration of PPAR-γ mRNA expression in myocytes. We made this conclusion because MCK-*Cre* transgene directed the recombination event to skeletal muscle cells, so the recombined transcript was only expressed in those cells.

Progressive insulin resistance in MKO mice

Body weights were similar in control and MKO mice at 6 and 14 months of age (**Table 1**). Basal glucose levels were measured every two months (data not shown); values were the same among all groups at 6 and 14 months of age (**Table 1**). Basal insulin levels, measured throughout the lifetime of these animals, were significantly elevated in MKO$^{fl/fl}$ compared with control$^{fl/fl}$ mice as early as 6 months of age ($P = 0.0004$). There was a nonsignificant increase in basal levels of free fatty acids (FFA; 20–25%) in both MKO groups, (and these differences were amplified during the glucose clamp study) (see below). Triglyceride levels were significantly elevated in both MKO groups compared with controls (~1.5-fold; $P = 0.001$) by 14 months of age (**Table 1**).

Table 1 Characteristics at baseline and during glucose clamp studies, at 6 and 14 months of age, with or without TZD treatment

Genotype	6 months untreated Control$^{fl/fl}$	6 months untreated MKO$^{fl/fl}$	14 months untreated Control$^{fl/fl}$	14 months untreated MKO$^{fl/fl}$	14 months untreated Control$^{fl/-}$	14 months untreated MKO$^{fl/-}$	14 months TZD-treated MKO
Body weight (g)	28 ± 1.1	33 ± 1.1	41 ± 2.8	44 ± 2.0	38 ± 4.0	43.7 ± 1.2	46.9 ± 1.5
Blood glucose (mg/dl)							
Basal	108 ± 6.47	123 ± 4.6	131 ± 5.6	139 ± 8.0	137 ± 7.0	134 ± 9.0	115 ± 4.6**
Clamp	140 ± 3.5	140 ± 2.1	148 ± 1.9	147 ± 2.06	148 ± 2.7	145 ± 6.3	146 ± 1.5
Insulin (ng/ml)							
Basal	0.6 ± 0.07	1.21 ± 0.12#	0.87 ± 0.2	1.5 ± 0.15#	0.81 ± 0.09	1.67 ± 0.3#	0.73 ± 0.1**
Clamp	9.9 ± 1.37	10.7 ± 0.58	9.4 ± 0.6	9.45 ± 1.2	8.2 ± 0.78	9.7 ± 1.4	8.6 ± 1.1
Plasma triglycerides (mg/dl)	85 ± 5.4	78 ± 2.5	135 ± 11	209 ± 16#	118 ± 12	200 ± 13#	117 ± 19**
Liver triglycerides (nmol/g)	—	—	6.3 ± 2	12.9 ± 3.5#	5.9 ± 2.4	11.1 ± 3.3#	34.8 ± 3.02**
Muscle triglycerides (nmol/g)	—	—	5.7 ± 2	8.4 ± 3.5	5.1 ± 2.4	7.8 ± 3	9.07 ± 1.77
Leptin (ng/ml)	4.8 ± 1.48	12.4 ± 2.1#	3.76 ± 1.0	4.0 ± 1.3	4.3 ± 0.32	11.6 ± 3.7#	
Acrp-30 (μg/ml)	25.4 ± 1.4	19.2 ± 1.28	21 ± 2.2	9.5 ± 1.6#	14 ± 1.4	8.8 ± 0.6#	25.5 ± 4.5**
Liver weight (g)	1.16 ± 0.06	1.12 ± 0.05	1.27 ± 0.12	1.5 ± 0.16	1.22 ± 0.09	1.84 ± 0.12#	1.9 ± 0.09*
Epididymal fat pad weight (g)	0.51± 0.07	1.17 ± 0.2#	1.4 ± 0.12	1.69 ± 0.08	1.11 ± 0.16	2.41 ± 0.3#	2.35 ± 0.18
Heart weight (g)	0.16 ± 0.015	0.14 ± 0.01	0.165 ± 0.02	0.196 ± 0.015	0.15 ± 0.008	0.174 ± 0.02	0.18 ± 0.01

Data for TZD-treated MKO animals was combined for simplicity. Biochemical parameters and tissue weights are represented as mean ± s.e.m. #, $P < 0.05$ for control versus MKO (within groups of like background); *, $P < 0.05$ for untreated MKO$^{fl/fl}$ versus TZD-treated MKO mice; **, $P < 0.05$ for both untreated versus TZD-treated MKO groups.

At 14 months, the absence of one *Pparg* allele in the control$^{fl/-}$ mice caused a significant reduction (33%; $P = 0.035$) in plasma Acrp-30 (adipocyte complement-related protein, 30 kDa). In addition, Acrp-30 levels in MKO$^{fl/fl}$ and MKO$^{fl/-}$ mice at 14 months of age was significantly lower than in control animals ($P = 0.0007$ and $P = 0.0197$, respectively).

At 6 months of age, circulating leptin levels and epididymal fat pad weight were both significantly elevated by more than twofold in MKO$^{fl/fl}$ compared with control$^{fl/fl}$ mice ($P = 0.026$ and $P = 0.02$, respectively); these differences were not seen at 14 months of age.

Insulin tolerance tests were done at 4, 8 and 12 months of age; data from the 4- and 12-month studies are shown (**Fig. 2a**,**b**). We have previously reported that animals heterozygous for *Pparg* deletion showed increased sensitivity to insulin[36] and, as expected, the control$^{fl/fl}$ and control$^{fl/-}$ animals showed normal and enhanced sensitivity, respectively. Unexpectedly, the ability of insulin to lower glucose levels was blunted in the MKO$^{fl/-}$ animals by 4 months of age (**Fig. 2a**; $P = 0.04$). An impaired response was also observed in MKO$^{fl/fl}$ compared with control$^{fl/fl}$ mice, and the effect was progressive and fully manifested at 12 months of age (**Fig. 2b**; $P = 0.001$). Intraperitoneal glucose tolerance tests done on the 12-month-old cohort confirmed that MKO$^{fl/fl}$ and MKO$^{fl/-}$ mice were glucose-intolerant and hyperinsulinemic compared with controls (**Fig. 2c**,**d**).

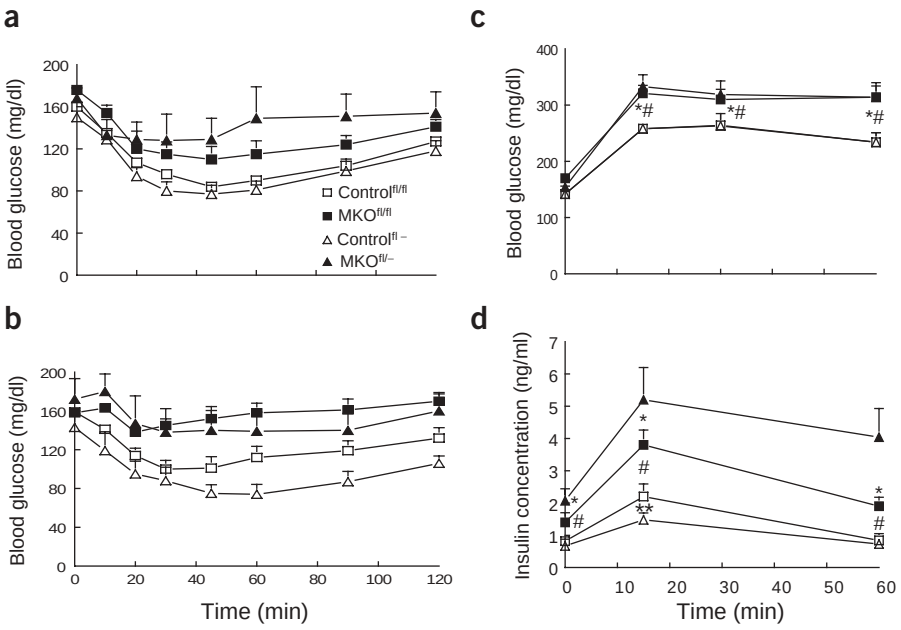

Figure 2 Insulin and glucose tolerance in MKO mice. (**a**,**b**) Insulin tolerance tests were conducted at 4 (**a**) and 12 (**b**) months of age. Glucose curves were significantly different between control$^{fl/-}$ and MKO$^{fl/-}$ mice ($P = 0.04$) at 4 months of age, and between control$^{fl/fl}$ and MKO$^{fl/fl}$ mice and between control$^{fl/-}$ and MKO$^{fl/-}$ mice ($P < 0.001$) at 12 months of age. (**c**,**d**) Glucose tolerance tests (**c**) and insulin curves (**d**) after glucose injection at 12 months of age. Values are expressed as mean ± s.e.m. $^{\#}$, $P < 0.05$ for control$^{fl/fl}$ versus MKO$^{fl/fl}$ mice; *, $P < 0.05$ for control$^{fl/-}$ versus MKO$^{fl/-}$ mice; **, $P < 0.05$ for control$^{fl/fl}$ versus control$^{fl/-}$ mice.

Pparg knockout in muscle affects insulin sensitivity

To quantitate *in vivo* insulin sensitivity in the four groups of mice at 6 and 14 months of age, animals were infused with 3-[^{3}H]glucose for 60 min and subjected to a two-step clamp using 6 and 12 mU/kg/min of human insulin. Deletion of *Pparg* in skeletal muscle led to a marked state of insulin resistance (**Fig. 3a**,**b**). The *in vivo* IS-GDR in MKO$^{fl/fl}$ and MKO$^{fl/-}$ mice showed substantial decreases of 25–45% ($P = 0.04$) at 6 months of age and 70–90% ($P < 0.01$) at 14 months of age, relative to control mice. Because most *in vivo* insulin-stimulated glucose disposal occurs in skeletal muscle, these data indicate insulin resistance and impaired glucose uptake in the muscle tissue of MKO mice.

To further localize this defect in insulin action directly to skeletal muscle, insulin-stimulated glucose transport was measured in

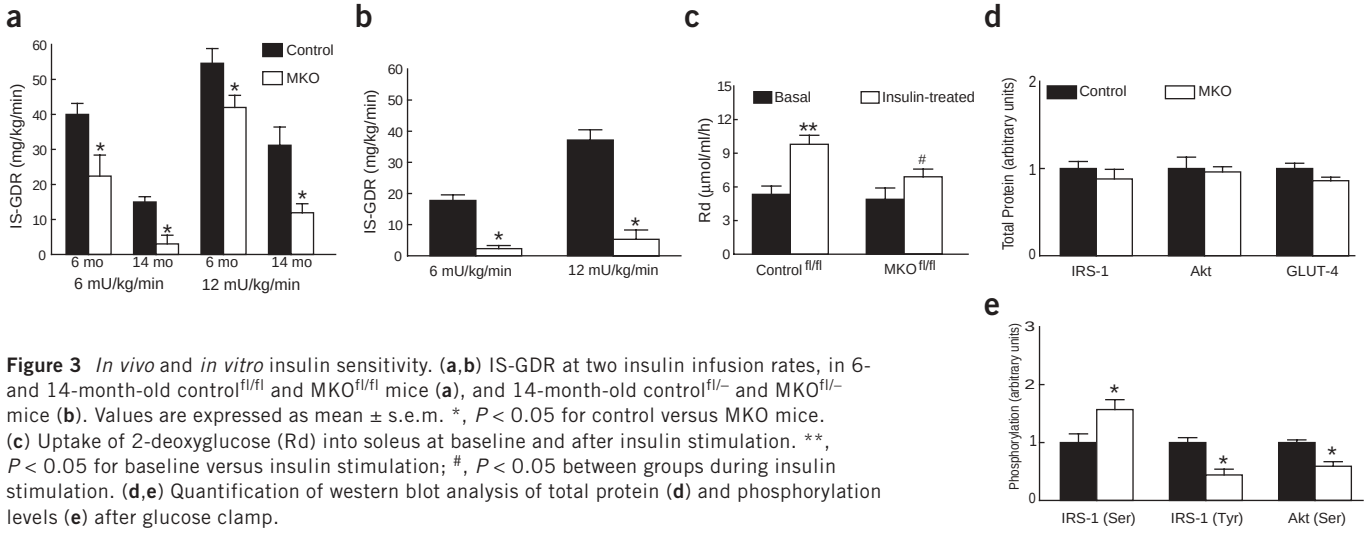

Figure 3 *In vivo* and *in vitro* insulin sensitivity. (**a**,**b**) IS-GDR at two insulin infusion rates, in 6- and 14-month-old control$^{fl/fl}$ and MKO$^{fl/fl}$ mice (**a**), and 14-month-old control$^{fl/-}$ and MKO$^{fl/-}$ mice (**b**). Values are expressed as mean ± s.e.m. *, $P < 0.05$ for control versus MKO mice. (**c**) Uptake of 2-deoxyglucose (Rd) into soleus at baseline and after insulin stimulation. **, $P < 0.05$ for baseline versus insulin stimulation; $^{\#}$, $P < 0.05$ between groups during insulin stimulation. (**d**,**e**) Quantification of western blot analysis of total protein (**d**) and phosphorylation levels (**e**) after glucose clamp.

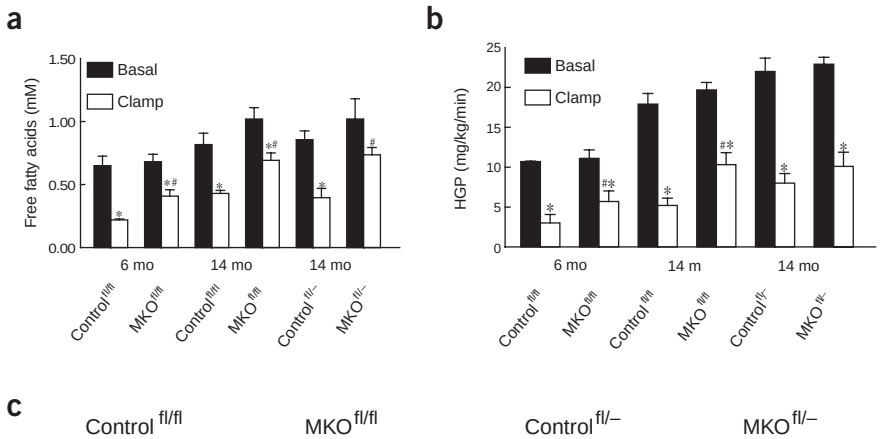

Figure 4 Effect of muscle *Pparg* deletion on adipose tissue and liver insulin sensitivity. (**a**,**b**) FFA levels (**a**) and HGP (**b**) at baseline and during clamp. Values are expressed as mean ± s.e.m. *, $P < 0.05$ for baseline versus clamp; #, $P < 0.05$ for control$^{fl/fl}$ versus MKO$^{fl/fl}$ or control$^{fl/-}$ versus MKO$^{fl/-}$ during insulin stimulation. (**c**) Hepatic lipid accumulation. Oil red O liver histology of control and MKO mice.

soleus muscle strips obtained from control$^{fl/fl}$ and MKO$^{fl/fl}$ mice. Glucose transport stimulation was severely blunted in soleus muscle from MKO$^{fl/fl}$ compared with control$^{fl/fl}$ mice (**Fig. 3c**; $P = 0.035$), providing further evidence of skeletal muscle insulin resistance, even when muscles are removed from the *in vivo* environment.

Measurement of GLUT-4 and insulin signaling molecules

Muscle samples were obtained at the end of the hyperinsulinemic-euglycemic clamp to determine the ability of the *in vivo* insulin infusion to activate the insulin signaling cascade in skeletal muscle. Using quantitative PCR, we found that mRNA expression levels for the insulin receptor, insulin receptor subtrate-1 (IRS-1), Akt and GLUT-4 were the same in muscle samples from control and MKO animals (data not shown). Similarly, western blots showed that expression of IRS-1, Akt, and GLUT-4 protein were the same between groups (**Fig. 3d**). It has been proposed that phosphorylation of IRS-1 at serine 307 decreases insulin-stimulated IRS-1 tyrosine phosphorylation, as well as IRS-1-mediated phosphatidylinositol-3-kinase signaling[37]. Using an antibody specific for phosphorylated serine 307, we found that IRS-1 serine phosphorylation was substantially increased (60%; $P = 0.027$; **Fig. 3e**) in MKO animals. Consistent with this, the ability of infused insulin to cause IRS-1 tyrosine phosphorylation was reduced by ~50% in MKO animals ($P = 0.005$), and Akt activation (as measured by phosphorylation of Akt serine 473) was similarly reduced ($P = 0.0006$).

Secondary insulin resistance in liver and adipose tissue

Steady-state circulating free fatty acid (FFA) levels represent a balance between FFA production and removal. The acute effects of insulin in lowering FFA levels are due, in large part, to insulin's antilipolytic effects in adipose tissue. In control animals, insulin infusion suppressed FFA levels by ~60% in both 6- and 14-month-old mice (**Fig. 4a**). This effect was significantly blunted in 6- and 14-month-old MKO$^{fl/fl}$ ($P = 0.0089$ and $P = 0.01$, respectively) mice, as well as 14-month-old MKO$^{fl/-}$ mice ($P = 0.009$), as fatty acid levels in those mice were depressed by only ~30%. These results indicate that a targeted change in PPAR-γ status in muscle can result in associated changes in adipose tissue.

Hepatic glucose production (HGP) was measured by infusion of [^{3}H]glucose. There were no differences in basal HGP rates between the groups (**Fig. 4b**). HGP was suppressed in all groups during the clamp, but insulin suppressed HGP by only 48% in MKO$^{fl/fl}$ mice compared to 72% ($P = 0.019$) in control$^{fl/fl}$ mice, indicating the exis-

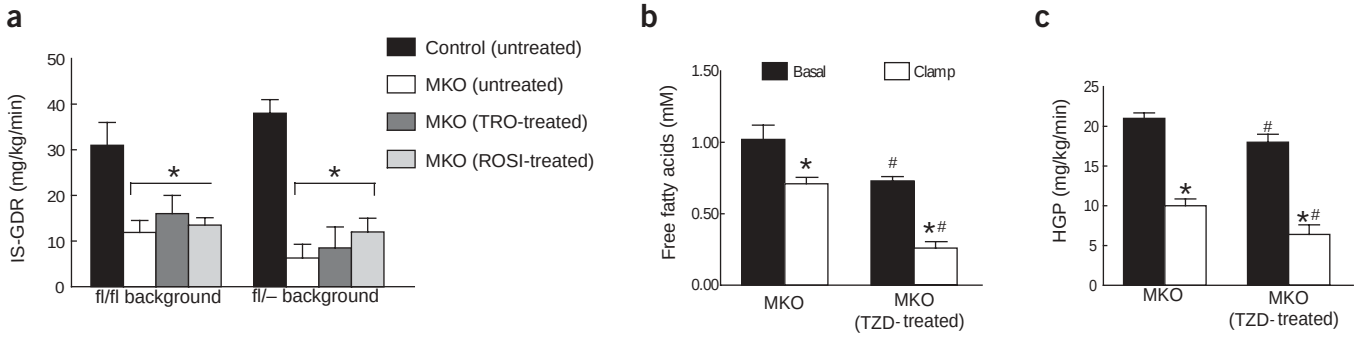

Figure 5 Effect of TZDs in MKO mice. (**a**) IS-GDR during clamp studies, before and after troglitazone (TRO) or rosiglitazone (ROSI) treatment. (**b**,**c**) Circulating FFA levels (**b**) and HGP (**c**) at baseline and after glucose clamp in untreated and TZD-treated MKO mice. FFA and HGP data from both TZD treatments and both MKO genotypes were combined for simplicity. *, $P < 0.05$ compared with baseline (within treatment group); #, $P < 0.05$ compared with untreated MKO mice (between treatment groups).

tence of hepatic insulin resistance. This suggests that the glucose intolerance in these animals (**Fig. 2c**), may be partly caused by inadequate suppression of HGP. The MKO$^{fl/-}$ mice seemed to be protected from the link between muscle PPAR-γ deletion and hepatic insulin resistance, as insulin-induced suppression of HGP was identical in both the control$^{fl/-}$ and MKO$^{fl/-}$ mice (**Fig. 4b**). Liver weights were somewhat increased in the Cre-expressing animals, and histologic sections (**Fig. 4c**) showed lipid droplet accumulation in hepatocytes from these mice.

Effects of TZD treatment in MKO mice

In vivo treatment of insulin resistance with TZDs causes insulin sensitization in skeletal muscle. These effects could be mediated by direct action of TZDs in muscle, or indirectly through action on another tissue, such as fat or liver, with secondary effects in muscle. To assess this issue, we treated MKO mice for 3 weeks with either troglitazone (0.2% food admixture) or rosiglitazone (3 mg per kg per d). TZD treatment did not enhance insulin-stimulated glucose disposal *in vivo* in the insulin-resistant MKO$^{fl/fl}$ or MKO$^{fl/-}$ animals (**Fig. 5a**). In addition, there was a 68% decrease (5.7 ± 2 versus 1.8 ± 0.7 μmol/g; $P = 0.035$) in intramuscular triglyceride content in control$^{fl/fl}$ animals, but no TZD-induced reduction in intramyocellular triglyceride content in MKO mice (**Fig. 5d**). Thus, animals lacking functional PPAR-γ in skeletal muscle do not show TZD-induced skeletal muscle insulin sensitization.

During the glucose clamp studies, we also measured circulating FFA levels (**Fig. 5b**) and HGP (**Fig. 5c**); because the effects of both TZDs were the same in the MKO animals (**Fig. 5b**), the data were combined. Basal FFA levels were elevated and poorly suppressed by insulin in the untreated MKO animals, whereas TZD administration decreased basal FFA levels below control values and enhanced the suppressive effects of insulin. In the untreated MKO animals, HGP was slightly elevated in the basal state, and the suppressive effects of insulin were significantly ($P = 0.019$) attenuated (**Fig. 5c**). After TZD treatment, basal HGP was decreased and the suppressive effects of insulin were restored ($P = 0.006$). TZDs also led to an increase of 2.9-fold ($P = 0.0001$) in intrahepatic triglyceride content, consistent with findings in other TZD-treated mouse models of insulin resistance[38]. Thus, TZDs exert their expected effects in adipose tissue and liver, but not muscle, in MKO animals.

Plasma glucose, insulin, triglyceride and FFA levels were all decreased *in vivo* in the TZD-treated animals (**Table 1**). Thus, despite the fact that TZD treatment did not improve insulin sensitization in skeletal muscle, most of the other symptoms of Syndrome X were ameliorated, highlighting the importance of adipose tissue and liver as target organs for TZDs.

Protein and gene expression measurements

Using quantitative PCR to measure mRNA expression of selected genes in skeletal muscle, we found that PPAR-α mRNA and AMPK protein levels were unchanged in MKO animals compared with controls, and were unaffected by TZD treatment (data not shown). Pyruvate dehydrogenase kinase-4 (PDK-4) and uncoupling protein-3 (UCP-3) mRNA levels were also comparable in MKO mice compared with controls (data not shown), but TZD administration caused a significant 85% decrease in UCP-3 and a 60% decrease in PDK-4 mRNA in all groups ($P = 0.0003$ and 0.02, respectively). This finding is consistent with a previous report[39] in which TZD treatment increased PDK-4 and UCP-3 mRNA in adipose tissue, but led to a decrease in mRNA in skeletal muscle; whether this effect was primary or secondary could not be determined. In the current study, we found that mRNA levels were equally decreased by TZDs in control and MKO mice. Because the MKO mice lack PPAR-γ in muscle, this suggests that the TZDs act indirectly in whole animals to decrease skeletal muscle PDK-4 and UCP-3 mRNA.

DISCUSSION

The well-known role of PPAR-γ in adipocyte function and differentiation and as the molecular target of antidiabetic TZDs suggests a specific role for adipose tissue in the etiology of the disease[6–12,39,40]. This view is strengthened by the observations that PPAR-γ is expressed at much higher levels in fat than in muscle, and that obesity is a primary risk factor for diabetes[13,23,33,40,41]. Despite these observations, muscle is the primary organ for insulin-stimulated glucose disposal[5,42], leading to the theory that *in vivo* insulin resistance cannot occur without a defect in muscle[42–44]. Using tissue-specific disruption of PPAR-γ expression, we showed that targeted loss of PPAR-γ in muscle results in a state of severe insulin resistance. The postprandial hyperglycemia, hyperinsulinemia and insulin resistance in targeted *Pparg* knockout mice from all ages provides the first direct evidence that PPAR-γ directly coordinates glucoregulatory responses in skeletal muscle.

The identification of muscle as a crucial tissue for PPAR-γ signaling raises the question of how this effect is achieved. Presumably this occurs, at least in part, through the regulation of specific target genes, although this muscle genetic network has not yet been identified. In addition, it seems that defects in muscle can lead to secondary adverse effects in liver and adipose tissue insulin action. Insulin resistance in hepatic and adipose tissue may be secondary to the hyperinsulinemia those animals exhibit, or it could reflect the paracrine influence of an unknown PPAR-γ-regulated secreted factor from muscle. Indeed, as a result of primary insulin resistance in muscle, PPAR-γ-deficient animals also developed hyperinsulinemia, glucose intolerance and hypertriglyceridemia. Taken together, all of these events recapitulate most of the manifestations of human Syndrome X, showing that a molecular defect causing insulin resistance in muscle can, over time, mimic most of the features of the human disease[43].

To evaluate potential cellular mechanisms of insulin resistance in MKO muscle, we measured the mRNA and/or protein expression levels of GLUT-4 and certain insulin signaling molecules. We found no differences in insulin receptor, IRS-1, Akt or GLUT-4 mRNA expression levels, or in IRS-1, Akt or GLUT-4 protein levels, in muscle samples from MKO and control animals. In contrast, significant defects in insulin signaling were observed when protein phosphorylation was measured. Serine phosphorylation of IRS-1 at position 307 inhibits insulin-stimulated IRS-1 tyrosine phosphorylation, blunting downstream insulin-mediated signaling[37]. Using a phospho-specific antibody, we found increased IRS-1 serine phosphorylation in the MKO samples, with a corresponding decrease in insulin-stimulated IRS-1 tyrosine phosphorylation and Akt activation. The decreases in these aspects of insulin signaling are consistent with the observed *in vivo* insulin resistance in the MKO animals, but we cannot yet determine whether these signaling defects are primary or secondary to the hyperinsulinemia, the elevated FFA levels or some other aspect of the insulin-resistant state.

We also treated the PPAR-γ-deficient animals with insulin-sensitizing TZDs. The results clearly show that TZD treatment did not augment insulin-stimulated GDR. Because the majority of GDR is accounted for by skeletal muscle uptake[5,42,44], it follows that TZD treatment did not enhance skeletal muscle insulin sensitivity in MKO animals. These results strongly argue that muscle PPAR-γ can be a direct target of TZDs *in vivo*. In the same animals, TZD treatment had

the expected effect of ameliorating hepatic and adipose tissue insulin insensitivity, indicating that the drugs remained fully effective through PPAR-γ in these tissues. Elevated FFA levels can lead to insulin resistance[4,5,10,41,42], so it is of interest that in MKO mice, TZD treatment lowered circulating FFA levels as a result of its effects on adipose tissue, even though no there was no insulin sensitization of skeletal muscle. This suggests that when intact animals and humans are treated with TZDs, the FFA-lowering action of these drugs on adipose tissue does not account for the insulin-sensitizing effects in muscle, and that direct actions of these drugs in muscle are needed.

Treatment of MKO animals with TZDs also resulted in lowered plasma glucose levels, normalization of hyperinsulinemia and reduced plasma triglyceride levels. This indicates that TZD treatment targeted to only adipose tissue and liver may be sufficient to normalize most of the major *in vivo* manifestations of Syndrome X. This approach allows us to begin a molecular dissection of the tissue-specific effects of TZDs in relation to their *in vivo* ability to normalize insulin resistance Metabolic Syndrome.

Changes in circulating Acrp-30 levels occurred in the MKO mice and could potentially affect metabolic physiology. Acrp-30 levels were lower in MKO than in control mice, and TZD treatment returned Acrp-30 to normal levels. In the face of this complete normalization of Acrp-30, we found that skeletal muscle insulin resistance in the MKO animals was still fully present and not at all ameliorated, indicating that the decrease in Acrp-30 was unlikely to be a cause of skeletal muscle insulin resistance. However, because hepatic and adipose tissue insulin resistance is secondary in these animals, it is possible that the decrease in circulating Acrp-30 may be a mechanistic factor, and TZD-induced normalization of Acrp-30 could contribute to the insulin sensitization effects observed, particularly in the liver.

In summary, the current study shows that selective deletion of PPAR-γ in muscle leads to a profound state of insulin resistance. This indicates that PPAR-γ operates directly as an important control point in skeletal muscle, regulating its capacity to respond to an insulin stimulus. Furthermore, the TZD treatment experiments indicate a role for muscle PPAR-γ as a direct target for the skeletal muscle insulin-sensitizing effects of these agents. Although the primary lesion in these mice is localized to skeletal muscle, a number of secondary and adaptive changes occur in the context of integrated, whole-animal *in vivo* physiology. These animals became hyperinsulinemic, glucose intolerant and hypertriglyceridemic. In addition, a moderate degree of insulin resistance developed in the non-skeletal muscle insulin target tissues, such as fat and liver. Thus, in the context of the whole animal, introducing insulin resistance into skeletal muscle leads to a variety of secondary and adaptive changes in other tissues which, when taken together, reproduce many of the manifestations characteristic of human Syndrome X.

METHODS

Creation of floxed, null and transgenic mice. Mice carrying null or floxed alleles of *Pparg* were created as described previously[36,45]. These mice were backcrossed to the C57BL/6J strain for eight generations. Mice were bred to create the following genotypes: $Pparg^{fl/fl}$ (control$^{fl/fl}$), $Pparg^{fl/fl}$MCK-*Cre* (MKO$^{fl/fl}$), $Pparg^{fl/-}$ (control$^{fl/-}$) and $Pparg^{fl/-}$MCK-*Cre* (MKO$^{fl/-}$). All experimental procedures were conducted in accordance with the Guide for Care and Use of Laboratory Animals of the National Institutes of Health, and were approved by the Animal Subjects Committee of the University of California, San Diego.

Phenotypic evaluation of mice. In the current investigation, we studied male control$^{fl/fl}$ ($n = 10$), MKO$^{fl/fl}$ ($n = 8$), control$^{fl/-}$ ($n = 10$) and MKO$^{fl/-}$ ($n = 6$) mice, with or without 3 weeks of TZD treatment (troglitazone in 0.2% food admixture or rosiglitazone, 3 mg per kg per d). Body weight measurements and fasting (6 h) plasma samples were obtained at 2, 4, 6, 8, 10, 12 and 14 months of age. Blood samples (~200 μl) were obtained by the tail-cut method. Whole blood was collected and the plasma withdrawn for subsequent analysis of glucose, FFAs, triglycerides, insulin, leptin and Acrp-30.

Insulin tolerance tests. At 4, 8, 10 and 12 months of age, animals were subjected to an insulin tolerance test. After a 6-h fast, a basal blood sample was taken, followed by intraperitoneal insulin injection (0.85 U/kg of Novolin R; Novo Nordisk Pharmaceutical Industries). Blood samples were drawn and measured for glucose at 15, 30, 45, 60, 90 and 120 min.

Glucose tolerance tests. At 12 months of age, glucose tolerance tests were conducted (1,000 mg/kg dextrose injected intraperitoneally; Abbott Laboratories) as previously described[36].

Euglycemic clamp studies. In two separate groups of mice, 6 and 14 months of age, animals were implanted with two catheters that were tunneled subcutaneously, exteriorized at the back of the neck and encased in silastic tubing, as previously described[36]. Four days after surgery, animals were fasted for 6 h and hyperinsulinemic-euglycemic clamps were done (see **Supplementary Methods** online). After the clamp, animals were killed and tissues (liver, epididymal fat, heart and skeletal muscle) were collected for subsequent analysis. Soleus muscle strips were excised from a separate set of control$^{fl/fl}$ and MKO$^{fl/fl}$ mice for *in vitro* assessment of insulin sensitivity, as previously described[46] (see **Supplementary Methods** online).

Chemical assays of blood, plasma or tissue. Plasma glucose concentration was measured with a HemoCue glucose analyzer. Insulin, leptin and Acrp-30 were measured using radioimmunoassay kits (Linco). Plasma triglycerides were measured using a Sigma Infinity triglyceride kit. Plasma glucose-specific activity was measured after deproteinization with barium hydroxide and zinc sulfate, as previously described by us[47]. Tissue triglycerides were extracted as previously described[48], and triglyceride content was determined by a GPO kit from ThermoDMA.

Liver histology. Liver samples were collected from 14-month-old mice from all four groups after the glucose clamp procedure. Samples were fixed in 10% neutral buffered formalin and embedded in paraffin. Sections were cut and subsequently stained with Oil Red O.

Western blot analysis. Red quadriceps muscle was homogenized in liquid nitrogen. Western blot analysis was used to assess protein and phosphorylation levels of GLUT-4 and various insulin signaling molecules. Immunoblots were expressed as arbitrary densitometry units, based on internal comparison with lysates prepared from control mice. Arbitrary densitometry units were quantified and are expressed as mean ± s.e.m.

RNA isolation. Frozen tissues were homogenized in TRIzol (Invitrogen) using a Polytron. RNA was precipitated with isopropanol, washed with 70% ethanol and resuspended in DEPC-treated water. Samples were subsequently frozen at –70 °C.

RT-PCR. Total RNA was extracted with TRIzol reagent (Gibco) from white adipose tissue, heart, skeletal muscle and liver of control and MKO mice, and subjected to RT-PCR to assess Cre activity (see **Supplementary Methods** online).

Quantitative PCR. 1 μl of 1:10 dilutions of the above RNA samples were used for quantitative PCR. Samples were run in triplicate in 10-μl reactions using an ABI 7700 (Applied Biosystems). RT-PCR samples were run once, and no amplification was observed. Amplification was done using SYBR Green technology (Applied Biosystems). Samples were incubated at 50 °C for 2 min and 95 °C for 10 min, followed by 40 cycles at 95 °C for 15 s and 60 ° C for 1 min. SYBR Green oligonucleotides were used to detect insulin receptor, IRS-1, Akt, GLUT-4, UCP-3, PPAR-α, PDK-4 and 36B4 (see **Supplementary Methods** online).

Calculations and statistical analyses. HGP and GDR were calculated as previously described[49]. Basal GDR was subtracted from total GDR to determine IS-GDR. ANOVA with Tukey *post-hoc* comparison were used to detect mean differences. Comparisons over time were determined using repeated-measures ANOVA. Values are presented as mean ± s.e.m. Significance was established at $P < 0.05$.

Note: Supplementary information is available on the Nature Medicine website.

ACKNOWLEDGMENTS

The authors thank J. Arimura and M. Nelson for assistance with animal care and husbandry; B. Hansen and E. Stevens for technical assistance with manuscript preparation; and C.R. Kahn for transgenic mice expressing MCK-*Cre*. These studies were supported by National Institutes of Health grants DK-33651 (J.M.O.), DK-60484 (A.L.H.), 2T32 DK07044-23 (W.H.) and DK57978-24 (R.M.E.), the National Institute for Diabetes, Digestive and Kidney Diseases, National Heart, Lung and Blood Institute grant HL56989 (R.M.E.), the Hilblom Foundation (J.M.O. and R.M.E.) and the Veterans Administration Research Service. R.M.E. is an investigator of the Howard Hughes Medical Institute at the Salk Institute for Biological Sciences.

COMPETING INTERESTS STATEMENT

The authors declare that they have no competing financial interests.

Received 29 August; accepted 2 October 2003
Published online at http://www.nature.com/naturemedicine

1. Harris, M.I. *et al.* Prevalence of diabetes, impaired fasting glucose, and impaired glucose tolerance in U.S. adults. The Third National Health and Nutrition Examination Survey. 1988–1994. *Diabetes Care* **21**, 518–524 (1998).
2. Meigs, J.B. Epidemiology of the metabolic syndrome. *Am. J. Manag. Care* **8**, S283–S292 (2002).
3. Reaven, G. Metabolic syndrome: pathophysiology and implications for management of cardiovascular disease. *Circulation* **106**, 286–288 (2002).
4. Suter, S.L., Nolan, J.L., Wallace, P., Gumbiner, B. & Olefsky, J. Metabolic effects of new oral hypoglycemic agent CS-045 in NIDDM subjects. *Diabetes Care* **15**, 193–203 (1992).
5. Saltiel, A.R. & Olefsky, J.M. Thiazolidinediones in the treatment of insulin resistance and type II diabetes. *Diabetes* **45**, 1661–1669 (1996).
6. Lehmann, J.M. *et al.* An anti-diabetic thiazolidinedione is a high affinity ligand for peroxisome proliferator-activated receptor γ. *J. Biol. Chem.* **270**, 12953–12956 (1995).
7. Ciaraldi, T.P., Gilmore, A. & Olefsky, J.M. *In vitro* studies on the action of CS-0455, a new anti-diabetic agent. *Metabolism* **39**, 1056-1062 (1990).
8. El-Kebbi, I., Rosner, S. & Pollet, R.J. Regulation of glucose transport by pioglitazone in cultured muscle cells. *Metabolism* **43**, 953–958 (1994).
9. Bowen, L., Steven, P.P., Stevenson, R. & Shulman, C.I. The effect of CP-68772, a thiazolidine derivative, on insulin sensitivity in lean and obese Zucker rats. *Metabolism* **40**, 1025–1030 (1991).
10. Fujiwara, T., Yoshioka, S., Yoshioka, T., Ushiyama, I. & Horikoshi, H. Characterization of new oral antidiabetic agent CS-045: studies in KK and ob/ob mice and Zucker fatty rats. *Diabetes* **37**, 1549–1558 (1998).
11. Kumar, S. *et al.* Troglitazone, an insulin action enhancer, improves metabolic control in NIDDM patients. *Diabetologia* **39**, 701–709 (1996).
12. Nolan, J.J., Ludvik, B., Beerdsen P., Joyce, M. & Olefsky, J. Improvements in glucose tolerance and insulin resistance in obese subjects treated with troglitazone. *N. Engl. J. Med.* **331**, 1188–1193 (1994).
13. Braissant, O., Foufelle, F., Scott, C., Dauce, M. & Wahli, W. Differential expression of peroxisome proliferator-activated receptors (PPARs): tissue distribution of PPAR-α, β and γ in the adult rat. *Endocrinology* **137**, 354–366 (1996).
14. Fajas, L. *et al.* Organization, promoter analysis and expression of the human PPARγ gene. *J. Biol. Chem.* **272**, 18779–18789 (1997).
15. Issemann, I. & Green, S. Activation of a member of the steroid hormone receptor superfamily by peroxisome proliferators. *Nature* **347**, 645–650 (1990).
16. Kliewer, S.A. *et al.* Differential expression and activation of a family of murine peroxisome proliferator-activated receptors. *Proc. Natl. Acad. Sci. USA* **91**, 7355–7359 (1994).
17. Spiegelman, B.M. PPARγ: adipogenic regulator and thiazolidinedione receptor. *Diabetes* **47**, 507–514 (1998).
18. Mangelsdorf, D.J. & Evans, R.M. The RXR heterodimers and orphan receptors. *Cell* **83**, 841–850 (1995).
19. Willson, T.M., Brown, P.J., Sternbach, D.D. & Henke, B.R. The PPARs: from orphan receptors to drug discovery. *J. Med. Chem.* **43**, 527–550 (2000).
20. Harris, P.K. & Kletzien, R.F. Localization of a pioglitazone response element in the adipocyte fatty acid-binding protein gene. *Mol. Pharamacol.* **45**, 439–445 (1994).
21. Auboeuf, D. *et al.* Tissue distribution and quantification of the expression of PPARs and LXRα in humans: no alterations in adipose tissue of obese and NIDDM patients. *Diabetes* **48**, 1319–1327 (1997).
22. Rosen, E.D. *et al.* PPARγ is required for the differentiation of adipose tissue *in vivo* and *in vitro*. *Mol. Cell* **4**, 611–617 (1999).
23. Tontonoz, P., Hu, E., Graves, R.A., Budavari, A.B. & Spiegelman, B.M. mPPAR-γ2: tissue-specific regulator of an adipocyte enhancer. *Genes Dev.* **8**, 1224–1234 (1994).
24. Vidal-Puig, A.J. *et al.* Peroxisome-proliferator-activated receptor gene expression in human tissues. Effects of obesity, weight loss, and regulation by insulin and glucocoticoids. *J. Clin. Invest.* **99**, 2416–2422 (1997).
25. Law, R.E. *et al.* Expression and function of PPARγ in rat and human vascular smooth muscle cells. *Circulation* **101**, 1311–1318 (2000).
26. Nagy, L., Tontonoz, P., Alvarez, J.G.A, Chen, H. & Evans, R.M. Oxidized LDL regulates macrophage gene expression through ligand activation of PPAR-γ. *Cell* **93**, 229–240 (1998).
27. Motojima, K., Passilly, P., Peters, J.M., Gonzalez, F.J. & Latruffe, N. Expression of putative fatty acid transporter genes are regulated by peroxisome proliferator-activated receptor α and γ activators in a tissue- and inducer-specific manner. *J. Biol. Chem.* **273**, 16710–16714 (1998).
28. Schoonjans, K., Staels, B. & Auwerx, J. The peroxisome proliferator activated receptors (PPARs) and their effects on lipid metabolism and adipocyte differentiation. *Biochim. Biophys. Acta* **1302**, 93–109 (1996).
29. Sears, I.B., MacGinnitie, M.A., Kovacs, L.G. & Graves, R.A. Differentiation-dependent expression of the brown adipocyte uncoupling protein gene: regulation by peroxisome proliferator activated receptor γ. *Mol. Cell Biol.* **16**, 3410–3418 (1996).
30. Tontonoz, P., Hu, E. & Spiegelman, B.M. Stimulation of adipogenesis in fibroblasts by PPARγ2, a lipid-activated transcription factor. *Cell* **79**, 1147–1156 (1994).
31. Young, P.W. *et al.* Repeat treatment of obese mice with BRL 49653, a new potent insulin sensitizer, enhances insulin action in white adipocytes: association with increased insulin binding and cell-surface GLUT4 as measured by photoaffinity labeling. *Diabetes* **44**, 1087–1092 (1995).
32. Wu, Z., Xie, Y., Bucher, N.L.R. & Farmer, S.R. PPARγ induces the insulin-dependent glucose transporter, GLUT4 in the absence of C/EBPα during the conversion of 3T3 fibroblasts into adipocytes. *J. Clin. Invest.* **101**, 22–32 (1998).
33. Loviscach, M. *et al.* Distribution of peroxisome proliferator-activated receptors (PPARs) in human skeletal muscle and adipose tissue: relation to insulin action. *Diabetologia* **43**, 304–311 (2000).
34. Barak, Y. *et al.* PPARγ is required for placental, cardiac and adipose tissue development. *Mol. Cell* **4**, 585–595 (1999).
35. Bruning, J.C. *et al.* A muscle-specific insulin receptor knockout exhibits features of metabolic syndrome of NIDDM without altering glucose tolerance. *Mol. Cell* **2**, 559–569 (1998).
36. Miles, P.D.G., Barak, Y., He, W., Evans, R.M. & Olefsky, J.M. Improved insulin-sensitivity in mice heterozygous for PPAR-γ deficiency. *J. Clin. Invest.* **105**, 287–292 (2000).
37. Lee, Y.H., Giraud, J., Davis, R.J. & White, M.F. c-Jun N-terminal kinase (JNK) mediates feedback inhibition of the insulin signaling cascade. *J. Biol. Chem.* **278**, 2896–2902 (2003).
38. Gavrilova, O. *et al.* Liver PPARγ contributes to hepatic steatosis, triglyceride clearance, and regulation of body fat mass. *J. Biol. Chem.* (in the press).
39. Way, J.M. *et al.* Comprehensive messenger ribonucleic acid profiling reveals that peroxisome proliferators activated receptor γ activation has coordinate effects on gene expression in multiple insulin sensitive tissues. *Endocrinology* **142**, 1269–1277 (2001).
40. Spiegelman, B.M. & Flier, J.S. Adipogenesis and obesity: rounding out the big picture. *Cell* **87**, 377–389 (1996).
41. Kahn, B.B. & Flier, J.S. Obesity and insulin resistance.*J. Clin. Invest.* **106**, 473–481 (2000).
42. DeFronzo, R.A., Bonadonna, R.C. & Ferrannini, E. Pathogenesis of NIDDM: a balanced overview. *Diabetes Care* **15**, 318–368 (1992).
43. Kido, Y. *et al.* Tissue-specific insulin resistance in mice with mutations in the insulin receptor, IRS-1, and IRS-2. *J. Clin. Invest.* **105**, 199–205 (1999).
44. Smith, D. *et al. In vivo* glucose metabolism in the awake rat: tracer and insulin clamp studies. *Metabolism* **36**, 1176–1186 (1987).
45. O'Goman, S., Dagenais, N.A., Qain, M. & Marchuk, Y. Protamine-Cre recombinase transgenes efficiently recombine target sequences in the male germ line of mice, but not in embryonic stem cells. *Proc. Natl. Acad. Sci. USA* **94**, 14602–14607 (1997).
46. Wilkes, J. & Bonen, A. Reduced insulin-stimulated glucose transport in denervated muscle is associated with impaired Akt-α activation. *Am. J. Physiol. Endocrinol. Metab.* **279**, E912–E919 (2000).
47. Revers, R.R., Fink, R., Griffin, J., Olefsky, J.M. & Kolterman, O.G. Influence of hyperglycemia on effects in type II diabetes. *J. Clin. Invest.* **73**, 664–672 (1984).
48. Frayn, K.N. & Maycock, P.F. Skeletal muscle triacylglycerol in the rat: methods for sampling and measurement, and studies of biological variability. *J. Lipid Res.* **21**, 139–144 (1980).
49. Steele, R. Influences of glucose loading and of injected insulin on hepatic glucose output. *Ann. NY Acad. Sci.* **82**, 420–430 (1959).